Veneziano, A, Meloro, C, Irish, JD, Stringer, C, Profico, A and De Groote, I

 Neuromandibular integration in humans and chimpanzees: implications for dental and mandibular reduction in Homo

http://researchonline.ljmu.ac.uk/id/eprint/8656/

Article

American Journal of
Physical Anthropology

WILEY

Neuromandibular integration in humans and chimpanzees: implications for dental and mandibular reduction in *Homo*.

SCHOLARONE™
Manuscripts

1
2
3
4
5
6
7
8
9
10
11
12
13
14
15
16
17
18
19
20
21
22
23
24
25
26
27
28
29
30
31
32
33
34
35
36
37
38
39
40
41
42
43
44
45
46
47
48
49
50
51
52
53
54
55
56
57
58
59
60

Neuromandibular integration in humans and chimpanzees: implications for dental and mandibular reduction in *Homo*.

Alessio Veneziano[1], Carlo Meloro[1], Joel D. Irish[1], Chris Stringer[2], Isabelle De Groote[1,2]

[1] School of Natural Sciences and Psychology, Liverpool John Moores University, Liverpool, L3 3AF, UK

[2] Department of Earth Sciences, The Natural History Museum, London, SW7 5BD, UK

Text pages: 15

Figures: 5

Tables: 2

Abbreviated title: Neuromandibular integration and lower jaw reduction in *Homo*

Key words: Dental reduction; Lower jaw; Neurocranium; Morphological integration; Geometric Morphometrics

Corresponding author:

Alessio Veneziano

School of Natural Sciences and Psychology, Liverpool John Moores University, Liverpool, L3 3AF, UK

veneziano.alessio@gmail.com

ABSTRACT

Objectives

Although the evolution of the hominin masticatory apparatus has been linked to diet and food processing, the physical connection between neurocranium and lower jaw suggests a role of encephalization in the trend of dental and mandibular reduction. Here, the hypothesis that tooth size and mandibular robusticity are influenced by morphological changes in the neurocranium was tested.

Materials and Methods

Three-dimensional landmarks, alveolar lengths and mandibular robusticity data were recorded on a sample of chimpanzee and human skulls. The morphological integration between the neurocranium and the lower jaw was analyzed by means of Singular Warps Analysis. Redundancy Analysis was performed to understand if the pattern of neuromandibular integration affects tooth size and mandibular robusticity.

Results

There was significant morphological covariation between neurocranium and lower jaw in both chimpanzees and humans. A positive relationship is evident between postcanine alveolar length and neurocranial length. Mandibular robusticity does not appear to be associated with morphological changes due to integration, except for symphyseal robusticity in humans.

Conclusions

The results of this study support the hypothesis that encephalization played a role in the trend of postcanine reduction in hominins and the origin of the peculiar anatomy of the mandibular symphysis of *Homo sapiens*. This study highlights the importance of structural constraints and non-adaptive factors on the evolution of the human and hominin skull.

1 INTRODUCTION

The human skull is the result of millions of years of morphological evolution involving all of its components. The increase in brain size, or encephalization, and the consequent changes in the size and shape of the neurocranium are the most prominent transformations in the hominin and human skull. *Homo sapiens* exhibits a brain size to body size ratio that is unparalleled among mammals (Herculano-Houzel, 2009; Leutenegger, 1982). In addition, a morphological reorganization from the elongated appearance of the brain in primates and Pleistocene hominins to a more globular shape occurred in *H. sapiens* (Lieberman et al., 2002). This reorganization is considered among the main factors contributing to the cognitive distinctiveness of modern humans (Holloway et al., 2009; Roth and Dicke, 2005). Beyond encephalization, other trends in the evolution of the skull contributed to human uniqueness. The reduction in dental and mandibular dimensions and robusticity (Brace, 1963; Emes et al., 2011; McHenry, 1982) is of particular importance for understanding hominin interactions with their environment. Indeed, food processing skills and changes in subsistence strategies have been proposed as pivotal to the reduction in tooth size and robusticity (Wrangham and Carmody, 2010; Zink and Lieberman, 2016). In addition, changes in the biomechanical stress on incisors has been hypothesized as the cause of the origin of the chin in *H. sapiens* (Daegling, 1993; Ichim et al., 2006). Since the main role of the lower jaw is food processing, it is not surprising that the main hypotheses concerning the trend of dental and mandibular reduction are linked to diet.

Although the neurocranium and lower jaw evolved under the influence of different factors, encephalization occurred almost simultaneously with dental and mandibular reduction (Jiménez-Arenas et al., 2014). Because of the physical connection between lower jaw and neurocranium, it is plausible to hypothesize a reciprocal influence between them. Indeed, structural modifications in one skeletal region may produce changes in other regions, a phenomenon referred to as morphological integration (Cheverud, 1982; Klingenberg, 2008). When integration occurs, the evolutionary meaning of morphological variability is difficult to assess; changes in one region may be simple by-products of changes in a contiguous region, and a trend that appears to be adaptive is actually a side effect of structural modifications on adjacent regions (Klingenberg, 2008). The lower jaw is connected to the cranium by the

temporomandibular joint; therefore, the mandible and teeth are potentially affected by structural changes triggered by modifications of neurocranial morphology (Bastir et al., 2005; Bookstein et al., 2003). Some authors argued that encephalization might have severely constrained the evolution of the skull (Bastir et al., 2010; Bruner and Ripani, 2008). In addition, the idea that some morphological changes in the lower jaw may be by-products of neurocranial evolution is supported from a developmental point of view. Indeed, in human ontogeny, the mandible is the last region of the skull to finish morphological development, following the cranial base, neurocranium and face respectively (Bastir et al., 2006). Thus, the neurocranium may substantially constrain the development of the mandible.

To determine if the trend of dental and mandibular reduction is affected by changes in the neurocranium, it is necessary to quantify the level of integration between these anatomical regions (neuro-mandibular integration) and to test for dependence between neurocranial morphology and lower jaw shape, size and robusticity. Analyzing the patterns of neuro-mandibular integration only in *H. sapiens* would not be sufficient to infer the causal relationship between dental/mandibular reduction and architectural reorganization of the neurocranium. A comparison between humans and related species is fundamental to understand whether: 1) the reduction in jaw robusticity and dental size is a by-product of the singular changes of the human neurocranium or 2) it is the effect of skull integration in other species as well.

In this study, the hypothesis that tooth size and mandibular robusticity in humans are influenced by morphological changes in the neurocranium was tested. Patterns of morphological integration between the neurocranium and the lower jaw were analyzed in a sample of *Pan troglodytes* and *H. sapiens*, by adopting a Geometric Morphometric approach. The relative influence that sex and allometry have on morphological integration between neurocranium and lower jaw was controlled throughout the analyses. In addition, correlations among the neuromandibular integration pattern, robusticity and dental size were analyzed to evaluate the link between neurocranial morphology and traits associated with mandibular and dental reduction in hominins.

1
2
3
4
5
6
7
8
9
10
11
12
13
14
15
16
17
18
19
20
21
22
23
24
25
26
27
28
29
30
31
32
33
34
35
36
37
38
39
40
41
42
43
44
45
46
47
48
49
50
51
52
53
54
55
56
57
58
59
60

2 MATERIALS AND METHODS

2.1 The sample and data collection

The sample in this study consists of 89 mandibles and matching crania belonging to *Pan troglodytes* (26 individuals, 14 females and 12 males) and *Homo sapiens* (63 individuals, 32 females and 31 males). The specimens belong to adult individuals of known sex. Full eruption of the third molar was used to estimate adulthood. The specimens of *P. troglodytes* are available from the online database of the Primate Research Institute at Kyoto University (KUPRI, Kyoto, Japan), from the primate skeletal collection of the National Museum of Natural History (NMNH, Washington, US) and from the Senckenberg Research Institute (Frankfurt, Germany). The human sample includes individuals of mixed populations from South East Asia, Oceania, Alaska, Greenland, and Black/White Americans curated at the NMNH and American Museum of Natural History (AMNH, New York, US); all are publicly available in CT-scan format (Copes, 2012).

The data consist of 3D coordinates, linear measurements, and metric indices from the surface renderings of specimens. A series of 28 3D landmarks was recorded on the mandibles and 15 landmarks on the neurocranium. Landmark configurations were recorded using the software Amira (version 5.4.5, Visualization Sciences Group), and chosen to describe overall morphology of the anatomical regions analyzed. A graphical representation of the landmarks is shown in Figure 1 and their definition is provided in Table 1. The landmarks of both configurations were aligned separately through a Generalized Procrustes Analysis (GPA) using Procrustes superimposition (Zelditch et al., 2012) to minimize the effect of size and spatial orientation. The resulting aligned configurations were used to extract size and shape information for mandibles and neurocrania of each individual. Centroid Size (CS) was used as a proxy for mandible and neurocranial size (Dryden and Mardia, 1998), and shape was approximated by the aligned 3D coordinates.

[Figure 1 here]

[Table 1 here]

Alveolar length and indices of mandibular robusticity were measured on mandibles and are shown in Figures 2 and 3. Alveolar length was used to approximate dental size of incisors (I_1-I_2), premolars (P_3-P_4) and molars (M_1-M_3). Alveolar lengths were measured as the minimum chord distances between midpoints of the interalveolar septa for each tooth type. Robusticity indices were calculated as the percent ratio between cross-section width and height (W/H x 100) of the mandibular corpus, measured at the symphysis (Rob SY) and below the first and second molars (Rob M_1 and Rob M_2). The cross-section of the symphysis was obtained as the intersection between the mandibular surface and mid-sagittal plane (identified by landmarks 1, 2 and 16 in Fig. 1). The cross-section of the mandibular corpus at the molars was obtained as the intersection between the mandibular surface and plane perpendicular to that identified by the alveolar points surrounding molars (landmarks 9, 10 and 11 for M_1, and 11, 12 and 13 for M_2). Height and width of each cross-section were used to calculate the robusticity indices (Fig. 3). The protocol for calculating robusticity indices on the virtual rendering of a mandible was developed in R (R Core Team, 2015).

[Figure 2 here]

[Figure 3 here]

2.2 Quantifying neuro-mandibular integration

Singular Warp (SW) analysis was performed to quantify the morphological integration between neurocranium and mandible. SW is a Partial Least Squares performed within a morphometric context (Bookstein et al., 2003). It computes the linear combinations of two sets of variables (two landmark sets) that have the highest mutual predictive power. SW produces vectors of shape variations and individual scores that maximize covariation between the two sets of landmarks analyzed, and provides an estimate of covariation (here referred to as Rpls) based on Pearson's correlation coefficient (Hollander et al., 2013). To calculate the significance of the integration test, the estimated value of integration is compared to the distribution of values obtained by randomly permuting the individuals

(1000 rounds of permutation). When the estimated covariation is larger than the permuted distribution, integration is significant (Bookstein et al. 2003). The first singular warp (SW1) was used to visualize the major shape covariation patterns between neurocranium and mandible. For each species, the mandible landmarks were aligned by Procrustes superimposition: the individuals showing the smaller Procrustes distance from the mean shape of their species were chosen for the visualization. The 3D surfaces of these specimens were warped to fit the landmark configuration of the mandible and neurocranial mean shape by using Thin Plate Spline (TPS) (Bookstein, 1989). The warped surfaces (now representing the species mean shapes) were warped along the SW1 using TPS. The resulting surfaces represent the shape covariation of mandible and neurocranium along the SW1. Singular Warps analysis and the TPS warping were performed in the R packages "geomorph" (Adams and Otárola-Castillo, 2013) and "Morpho" (Schlager, 2013) respectively.

2.3 Redundancy analysis

Redundancy Analysis (RDA) (Legendre and Legendre, 2012) is a statistical ordination method to extract the unique and shared contributions of a set of independent variables (explanatory variables) on a set of dependent variables (response variables). It uses multiple linear regressions to extrapolate a matrix of predicted values that are then ordinated by Principal Component Analysis. RDA provides the unique and shared contributions of the independent on the dependent variables as values of adjusted R^2. The shared contribution is the percentage of variance of the dependent variable that is contemporarily explained by two or more independent variables together. The unique contribution is the variance explained by each independent variable when their shared contributions are removed. RDA was performed on each species to determine the relative influence of sex (dimorphism), size (allometry) and the neuro-mandibular covariation pattern to the variance of mandibular shape. The shape of the mandible consisted of a matrix of individual PC scores extracted from the PCA performed on the mandibular landmarks. The mandible SW scores of the first singular warp were used as a proxy of the pattern of neuro-mandibular covariation. Sex and the Centroid Size of the landmark configurations of the mandible were used as additional independent variables. To understand if the integration between mandible and neurocranium could affect mandibular and dental reduction, RDA was also performed on

alveolar lengths and robusticity indices (dependent variables). Sex and mandibular Centroid Size were used as additional independent variables. The RDA was performed by using the R package "vegan" (Dixon, 2003).

3 RESULTS

3.1 Shape integration

Singular Warp analysis revealed a significant pattern of integration between mandible and neurocranium in both humans and chimpanzees. The shape variations associated with the first singular warp are shown in Figure 4. In *P. troglodytes*, the integration between mandible and neurocranium (Rpls: 0.82, p: 0.004) accounts for the covariation between cranial vault relative length, zygomaticomaxillary height, mandibular corpus height and ramus breadth. In particular, a shorter vault and vertically extended zygomaticomaxillary suture are accompanied by the increase in mandibular corpus height and the reduction of ramus breadth (Fig. 4). As a result of cranial elongation, the zygomatic arch is also stretched antero-posteriorly. In addition, shortening of the neurocranium is associated with slight changes in the size of mandibular condyles, which are larger in elongated vaults (Fig. 4). In *H. sapiens*, a significant pattern of neuromandibular integration was found (Rpls: 0.64, p: 0.019). The variations from elongated to shortened cranial vaults are associated with the reduction of mandibular corpus height at the level of molars and an increase at the symphysis. The cranial vault shortening is furthermore correlated with an increase in ramus breadth and the reduction of the gonial angle. As a result, the mandibular ramus projects increasingly backward when neurocranium extends antero-posteriorly, leaving a wider space to accommodate the third molar (Fig. 4).

[Figure 4 here]

3.2 Tooth size, mandibular robusticity and integration

The redundancy analysis showed that the pattern of neuromandibular integration explains significant fractions of the overall mandibular shape variance in both humans and chimpanzees. The results of the redundancy analysis are shown in Table 2. In *P. troglodytes*, 17% (p: 0.001) of the total shape variance of the mandible is explained by neuromandibular integration and sex and size do not contribute to this percentage. In *H. sapiens*, 16% of mandibular shape variance is affected by neuromandibular integration (p: 0.001), and the contribution of sex and size is negligible (nearly 0%).

Metric data of alveolar lengths and robusticity were used to determine the effect of neurocranial shape on the measurements traditionally linked to dental and mandibular reduction. Figure 5 shows scatterplots and linear correlations between alveolar lengths, robusticity and the pattern of neuromandibular integration, when significant.   In *P. troglodytes*, changes in premolar (Variance: 26%, p: 0.004) and molar (Variance: 38%, p: 0.002) alveolar lengths correlate with neuromandibular integration. In premolars, sex and size contribute to the variance explained by integration by 3%; therefore, the unique contribution of integration is 26%. Both premolars and molars increase in size when the neurocranium lengthens (Fig. 4). The neuromandibular integration in *H. sapiens* was found to correlate with incisor (Variance: 5%, p: 0.046), premolar (Variance: 13%, p: 0.002), and molar (Variance: 8%, p: 0.018) alveolar lengths, and robusticity measured at the symphysis (Variance: 17%, p: 0.002). Sex and size have minor contributions to the variance explained by integration in the case of premolars (Variance: 1%) and molars (Variance: 1%). Figure 5 shows that an inverse relationship exists between incisor alveolar length and neurocranial length, while symphyseal robusticity, premolar and molar alveolar lengths increase when neurocranium lengthens (Fig. 4).

[Table 2 here]

[Figure 5 here]

1
2
3
4
5
6
7
8
9
10
11
12
13
14
15
16
17
18
19
20
21
22
23
24
25
26
27
28
29
30
31
32
33
34
35
36
37
38
39
40
41
42
43
44
45
46
47
48
49
50
51
52
53
54
55
56
57
58
59
60

4 DISCUSSION

4.1 The neurocranium as a constraint

The physical connection between skull regions implies a certain level of mutual influence on their development and evolution (Bastir et al., 2010; Klingenberg, 2008). Therefore, it is not surprising that the neurocranium and mandible display significant morphological integration in both humans and chimpanzees in the present analysis. Nevertheless, this pattern has never received explicit consideration, although other authors have recognized the presence of morphological integration between mandibular ramus and temporal bone (Bastir et al., 2004). The results presented above show that shape changes in the neurocranium can affect mandibular morphology, a pattern shared by both humans and chimpanzees. The length of the cranial vault seems to play a pivotal role in the pattern of neuromandibular integration. Morphological changes in the zygomatic bone are also involved, in particular in *P. troglodytes*. The covariation between the lower jaw and zygomatic region may appear to be associated with biomechanical differences because of changes in the size and orientation of masseter attachments. Previous studies on cranial integration (Singh et al., 2012) found that the expansion of the posterior cranial vault is associated with enlargement and reorientation of the zygomatics in great apes. Although these changes in the zygomatic bone could be biomechanically relevant, they may arise as a by-product of cranial integration. This perspective is supported by the ontogenetic relationship between neurocranium and face, the former finishing its morphological development earlier than the latter (Bastir et al., 2006). These findings suggest that the neurocranium may act as a structural constraint to the lower jaw (and to the skull in general) during ontogeny.

4.2 The chimpanzee skull as a model of hominin integration

Some traits of the lower jaw and neurocranium change accordingly in different species (Fig. 4, Table 2). In both *H. sapiens* and *P. troglodytes*, postcanine alveolar lengths seem to

respond similarly to common changes in neurocranial shape. Nevertheless, more features follow a reverse trend. Indeed, a shortened neurocranium is associated with reduced ramus breadth and a taller corpus in chimpanzees, which is opposite the condition in humans. In addition, changes in some mandibular traits in humans, such as gonial angle, are unparalleled in chimpanzees (Fig. 4). These results indicate that the structural relationship between the neurocranium and mandible cannot be generalized. The integration between these anatomical regions does not necessarily produce similar responses to similar shape changes. Therefore, the way neuromandibular integration affects lower jaw morphology in humans cannot be seen as a general response to neurocranial shortening, but rather the effect of the singular shape changes of the human neurocranium (Herculano-Houzel, 2009; Lieberman et al., 2002). Consequently, *H. sapiens* may not be a good model for the study of neuromandibular integration in hominins. Because of the shared cranial lengthwise development of non-human hominins and chimpanzees (Lieberman et al., 2002), *P. troglodytes* may be better suited than humans for the analyses of neurocranial constraints to the hominin lower jaw

4.3 Integration and the trend of reduction

The covariation between neurocranial shape and postcanine alveolar lengths has important implications for the evolution of the lower jaw. The reduction of postcanine tooth size is considered among the major trends in the evolution of the hominin skull (Emes et al., 2011; McHenry, 1982). Previous studies (Jiménez-Arenas et al., 2014) found an inverse relationship between encephalization and postcanine tooth size in *Homo* and rejected the link between diet and changes in molar and premolar size. The results above support previous findings that changes in brain size (and consequent shape alterations of the neurocranium) affect the size of postcanine dentition (Figs. 4-5). In fact, the pattern of neuromandibular integration was found to correlate positively with molar and premolar alveolar lengths in both *P. troglodytes* and *H. sapiens*. Based on the results above, the neuromandibular integration pattern observed in chimpanzees suggests that neurocranial changes across hominins may have influenced the size of postcanine dentition. Although

brain enlargement may have triggered improvements in cognitive skills of extraoral food processing, thus making larger premolars and molars unnecessary (Ross et al., 2009), the structural relationship between neurocranium and postcanine teeth allows for a more parsimonious explanation of dental reduction. The correlation between postcanine alveolar length and neuromandibular integration within *H. sapiens* suggests that the neurocranium may have acted as a constraint also in the human trend of reduction during the Holocene (Brace and Mahler, 1971).

Previous studies addressed the hypothesis of a link between encephalization and dental reduction by looking exclusively at postcanine dentition (Gómez-Robles et al., 2017; Jiménez-Arenas et al., 2014). Nevertheless, incisor size and mandibular robusticity were just as important in the evolution of the genus *Homo*. In this study, neuromandibular integration in *H. sapiens* was found to have a significant influence on incisor alveolar length, which decreases when neurocranial length increases (Fig. 5). Although significant, this relationship is not highly relevant, because neuromandibular integration explains only a small variance of incisor alveolar length (Table 2). In addition, this relationship does not hold in *P. troglodytes*, so may not be applicable to non-human hominins (see section 4.2).

Robusticity is approximated by the width to height ratio of the mandibular corpus and it is known for its role in counteracting torsional and bending forces during mastication in primates (Hylander, 1985). Increases in corpus height result in a reduction of mandibular robusticity, as observed in the evolution of the genus *Homo* (Chamberlain & Wood, 1985). The pattern of neuromandibular integration seems to involve changes in the height of mandibular corpus in both humans and chimpanzees (Fig. 4). Nevertheless, the results of the Redundancy Analysis do not support the hypothesis that variations in robusticity are subject to changes in the shape of the neurocranium (Table 2). The only exception is represented by symphyseal robusticity in *H. sapiens*, which holds a positive relationship with neurocranial length (Fig. 5). Among hominins, *H. sapiens* exhibits a unique anatomy of the mandibular symphysis, as the only species with a forward projecting chin (Schwartz & Tattersall, 2000). This attribute led researchers to hypothesize a biomechanical role for the human chin (Daegling, 1993; Ichim et al., 2006), also based on the observation of its correlation with dietary proxies in other primates (Begun et al., 2013; Demes et al., 1984; Hylander, 1985). The results above suggest that the morphology of the human

neurocranium may be the cause of the reduced robusticity observed in the chin. Because of the reorganization of the neurocranium to a "globular" shape in *H. sapiens* (Lieberman et al., 2002), the mandibular symphysis may be constrained in a lengthwise direction during ontogeny. The absence of a relationship between symphyseal robusticity and neuromandibular integration in *P. troglodytes* also supports that the neurocranial constraint on the chin is due to the singular reorganization of the head in *H. sapiens*.

The results above support the hypothesis that the postcanine tooth size reduction in hominins and evolution of the mandibular symphysis in *H. sapiens* were under the influence of neurocranial shape changes. This hypothesis does not hold for incisors and mandibular robusticity at molars, which likely evolved in response of changes in biomechanical requirements. Future studies will address the neuromandibular integration in an ontogenetic perspective, to clarify the tempo and mode of mutual interaction between neurocranium and lower jaw in humans. The results of this work suggest that structural, non-adaptive factors had a larger influence on human morphological evolution than previously thought.

ACKNOWLEDGMENTS

LITERATURE CITED

Adams, D. C., & Otárola-Castillo, E. (2013). geomorph: an R package for the collection and analysis of geometric morphometric shape data. Methods in Ecology and Evolution, 4:393-399.

Bastir, M., Rosas, A., & Kuroe, K. (2004). Petrosal orientation and mandibular ramus breadth: Evidence for an integrated petroso-mandibular developmental unit. American Journal of Physical Anthropology, 123:340-350.

Bastir, M., Rosas, A., & O'Higgins, P. (2006). Craniofacial levels and the morphological maturation of the human skull. Journal of Anatomy, 209:637-654.

Bastir, M., Rosas, A., & Sheets, H. D. (2005). The morphological integration of the hominoid skull: a partial least squares and PC analysis with implications for European Middle Pleistocene mandibular variation. In Slice, E. D. (Ed.), Modern morphometrics in physical anthropology. Kluwer Academic/Plenum Publishers, New York.

Bastir, M., Rosas, A., Stringer, C., Cuétara, J. M., Kruszynski, R., Weber, G. W., Ross, C. F., & Ravosa, M. J. (2010). Effects of brain and facial size on basicranial form in human and primate evolution. Journal of Human Evolution, 58:424-431.

Begun, D. R., Ward, C. V., & Rose, M. D. (2013). Function, phylogeny, and fossils: Miocene hominoid evolution and adaptations. Springer Science & Business Media, New York.

Bookstein, F. L. (1989). Principal warps: Thin-plate splines and the decomposition of deformations. IEEE Transactions on pattern analysis and machine intelligence, 11:567-585.

Bookstein, F. L., Gunz, P., Mitterœcker, P., Prossinger, H., Schæfer, K., & Seidler, H. (2003). Cranial integration in Homo: singular warps analysis of the midsagittal plane in ontogeny and evolution. Journal of Human Evolution, 44:167-187.

Brace, C. L. (1963). Structural reduction in evolution. The American Naturalist, 97:39-49.

Brace, C. L., Mahler, P. E. (1971). Post-Pleistocene changes in the human dentition. *American Journal of Physical Anthropology*, 34:191-203.

Bruner, E., Ripani, M. (2008). A quantitative and descriptive approach to morphological variation of the endocranial base in modern humans. *American Journal of Physical Anthropology*, 137:30-40.

Chamberlain, A. T., Wood, B. A. (1985). A reappraisal of variation in hominid mandibular corpus dimensions. *American Journal of Physical Anthropology*, 66:399-405.

Cheverud, J. M. (1982). Phenotypic, genetic, and environmental morphological integration in the cranium. *Evolution*, 36:499-516.

Copes, L. (2012). Comparative and experimental investigations of cranial robusticity in mid-Pleistocene hominins. (Ph.D. Dissertation). Anthropology, Arizona State University, Tempe, Arizona.

Daegling, D. J. (1993). Functional morphology of the human chin. *Evolutionary Anthropology*, 1:170-177.

Demes, B., Preuschoft, H., Wolff, J. E. A. (1984). Stress-strength relationships in the mandibles of hominoids. In Chivers, D. J., Wood, B. A., Bilsborough, A. (Eds.), *Food acquisition and processing in primates*. Springer Science & Business Media, New York.

Dixon, P. (2003). VEGAN, a package of R functions for community ecology. *Journal of Vegetation Science*, 14:927-930.

Dryden, I. L., Mardia, K. V. (1998). *Statistical analysis of shape*. John Wiley & Sons, Hoboken.

Emes, Y., Aybar, B., Yalcin, S. (2011). On the evolution of human jaws and teeth: A review. *Bulletin of the International Association for Paleodontology*, 5:37-47.

Gómez-Robles, A., Smaers, J. B., Holloway, R. L., Polly, P. D., Wood, B. A. (2017). Brain enlargement and dental reduction were not linked in hominin evolution. *Proceedings of the National Academy of Sciences of the United States of America*, 114:468-473.

Herculano-Houzel, S. (2009). The human brain in numbers: A linearly scaled-up primate brain. *Frontiers in Human Neuroscience*, 3:1-11.

Hollander, M., Wolfe, D. A., Chicken, E. (2013). *Nonparametric statistical methods*. John Wiley & Sons, Hoboken.

Holloway, R. L., Sherwood, C. C., Hof, P. R., Rilling, J. K. (2009). Evolution of the brain in humans: Paleoneurology. In Binder, M. D., Hirokawa, N., Windhorst, U. (Eds.), *Encyclopedia of neuroscience*. Springer, Berlin.

Hylander, W. L. (1985). Mandibular function and biomechanical stress and scaling. *American Zoologist*, 25:315-330.

Ichim, I., Swain, M., Kieser, J. A. (2006). Mandibular biomechanics and development of the human chin. *Journal of Dental Research*, 85:638-642.

Jiménez-Arenas, J. M., Pérez-Claros, J. A., Aledo, J. C., Palmqvist, P. (2014). On the relationships of postcanine tooth size with dietary quality and brain volume in Primates: Implications for hominin evolution. *BioMed Research International*. doi: 10.1155/2014/406507.

Klingenberg, C. P. (2008). Morphological integration and developmental modularity. *Annual Review of Ecology, Evolution, and Systematics*, 39:115-132.

Legendre, P., Legendre, L. F. (2012). *Numerical ecology*. 3rd English ed. Elsevier, Amsterdam.

Leutenegger, W. (1982). Encephalization and obstetrics in primates with particular reference to human evolution. In Armstorong, E., Falk, D. (Eds.), *Primate brain evolution: Methods and concepts*. Plenum Publishing, New York.

Lieberman, D. E., McBratney, B. M., Krovitz, G. (2002). The evolution and development of cranial form in Homo sapiens. *Proceedings of the National Academy of Sciences of the United States of America*, 99:1134-1139.

McHenry, H. M. (1982). The pattern of human evolution: studies on bipedalism, mastication, and encephalization. *Annual Review of Anthropology*, 11:151-173.

R Core Team (2015). R: A language and environment for statistical computing. *R Foundation for Statistical Computing*, Vienna, Austria. URL http://www.R-project.org/.

Ross, C. F., Washington, R. L., Eckhardt, A., Reed, D. A., Vogel, E. R., Dominy, N. J., Machanda, Z. P. (2009). Ecological consequences of scaling of chew cycle duration and daily feeding time in Primates. *Journal of Human Evolution*, 56:570-585.

Roth, G., Dicke, U. (2005). Evolution of the brain and intelligence. *Trends in Cognitive Sciences*, 9:250-257.

Schlager, S. (2013). Morpho: Calculations and visualizations related to Geometric Morphometrics. R package version 0.17. http://sourceforge.net/projects/morpho-rpackage/

Schwartz, J. H., Tattersall, I. (2000). The human chin revisited: What is it and who has it? *Journal of Human Evolution*, 38:367-409.

Singh, N., Harvati, K., Hublin, J. J., Klingenberg, C. P. (2012). Morphological evolution through integration: a quantitative study of cranial integration in *Homo*, *Pan*, *Gorilla* and *Pongo*. *Journal of Human Evolution*, 62:155-164.

Wrangham, R., (2009). *Catching fire: How cooking made us human*. Basic Books. New York.

Wrangham, R., Carmody, R. (2010). Human adaptation to the control of fire. *Evolutionary Anthropology*, 19:187-199.

Zelditch, M. L., Swiderski, D. L., Sheets, H. D. (2012). *Geometric morphometrics for biologists: a primer*. Academic Press, New York.

Zink, K. D., Lieberman, D. E. (2016). Impact of meat and Lower Palaeolithic food processing techniques on chewing in humans. *Nature*. 531:500-503.
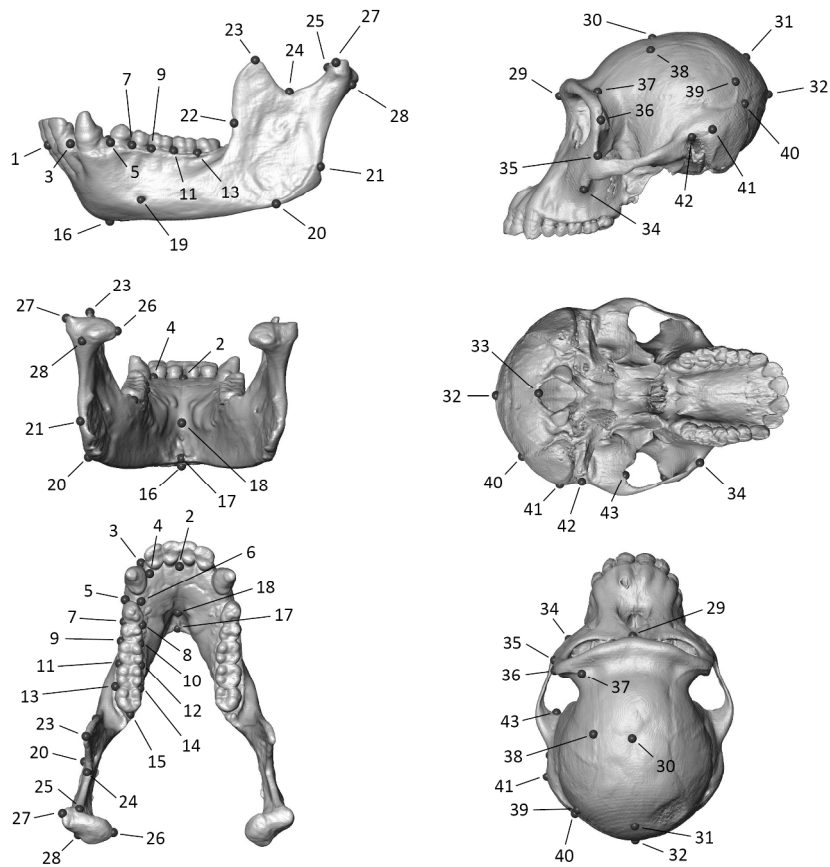
Landmark configurations on the mandible (left, 1-28) and the neurocranium (right, 29-43), shown on the mandible and neurocranium of a female Pan troglodytes. The landmarks are defined in Table 1. The enumeration follows the table of definitions.

766x670mm (96 x 96 DPI)
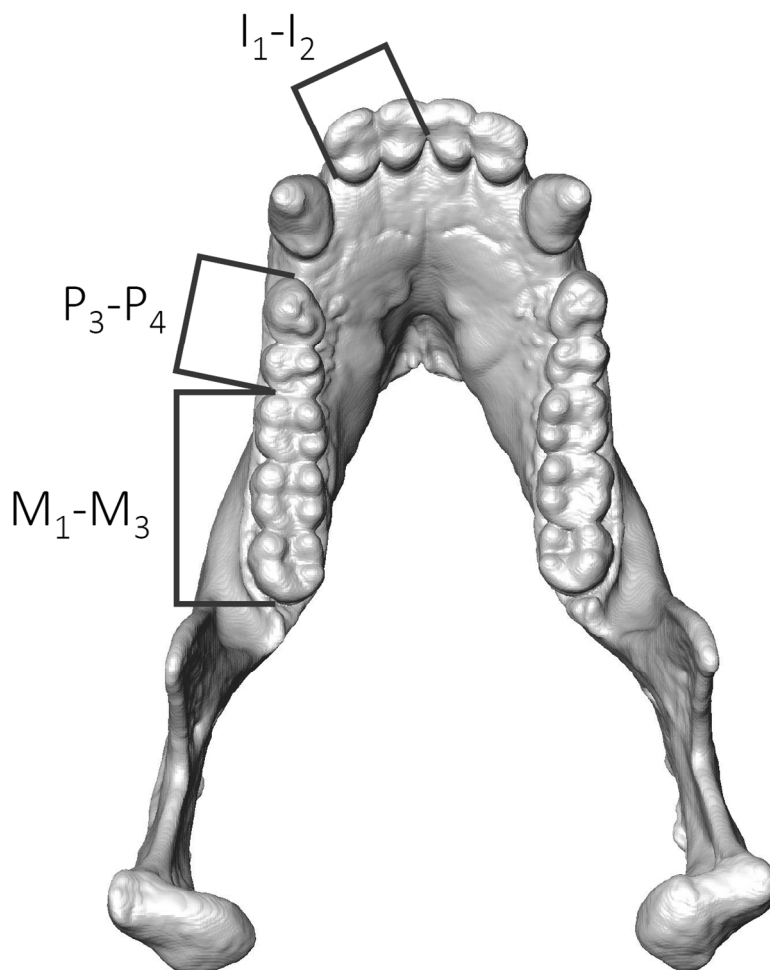
Alveolar lengths of incisors (I1-I2), premolars (P3-P4) and molars (M1-M3) shown on the mandible of a female Pan troglodytes. Alveolar lengths were measured as the minimum chord distances between midpoints of the interalveolar septa.

397x510mm (96 x 96 DPI)

1
2
3
4
5
6
7
8
9
10
11
12
13
14
15
16
17
18
19
20
21
22
23
24
25
26
27
28
29
30
31
32
33
34
35
36
37
38
39
40
41
42
43
44
45
46
47
48
49
50
51
52
53
54
55
56
57
58
59
60
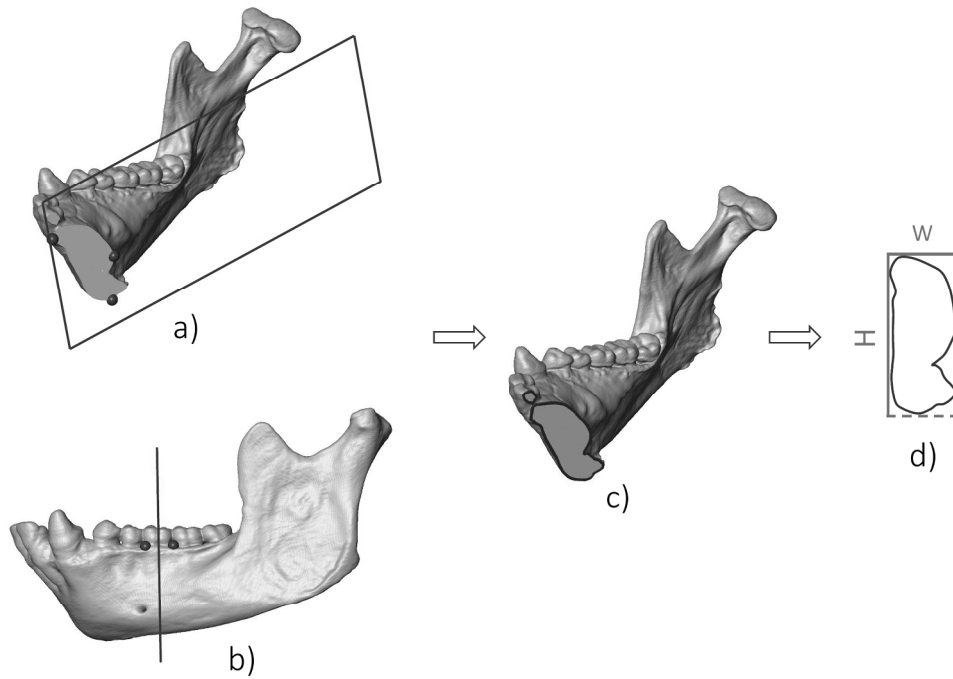
Computational procedure for the extrapolation of robusticity indices, shown on the mandible of a female Pan troglodytes. Three landmarks were used to define (a) the sagittal plane for intersecting the symphysis and (b) a plane orthogonal to the alveolar plane to intersect the mandible at the M1 and M2 (not shown). The intersection (c) provides a bi-dimensional profile of the mandible (d), whose main axes represent mandibular corpus height (H) and width (W).

607x446mm (96 x 96 DPI)
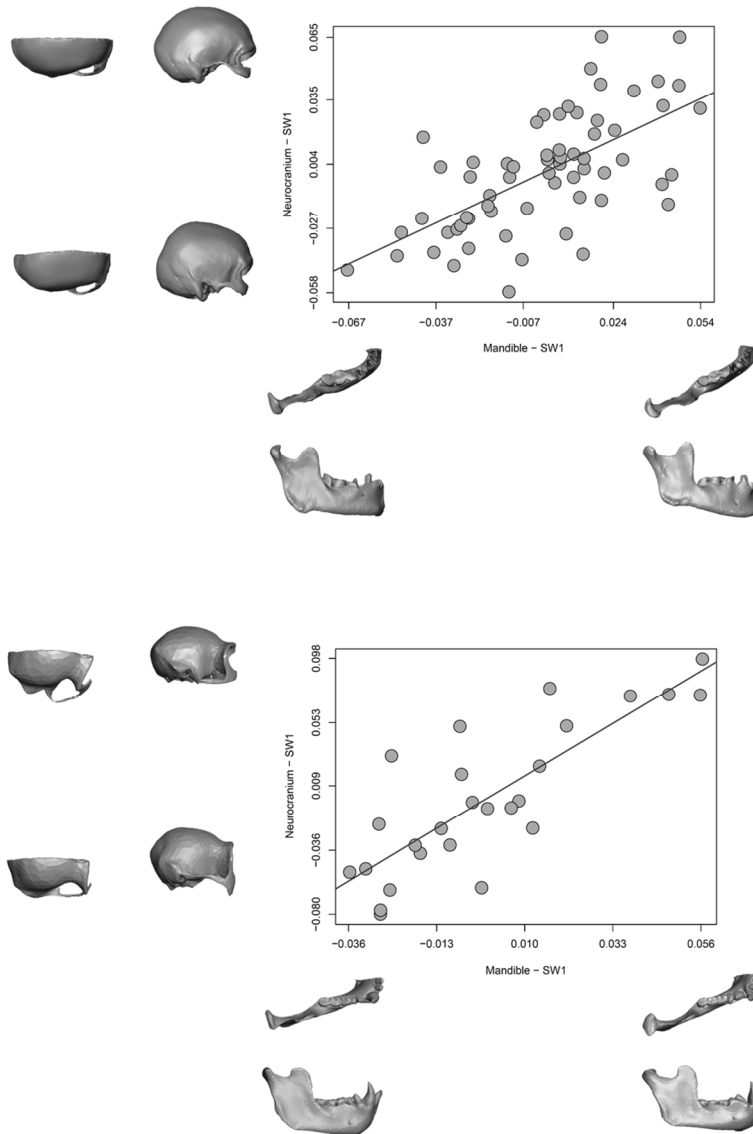
First Singular Warp (SW1) maximising the covariation between neurocranium (Y axis) and mandibular (X axis) shapes in Pan troglodytes (below) and Homo sapiens (above). The shape variations of mandible and neurocranium along the SW1 are shown as Thin-Plate-Spline warped surfaces, and are displayed along the respective axes. The differences along one axis represent the shape variations associated with the changes in shape along the other axis. Each surface corresponds to the shape at minimum and maximum of its axis. The warped surfaces show how changes in the neurocranium influence the shape of the mandible.

299x417mm (96 x 96 DPI)
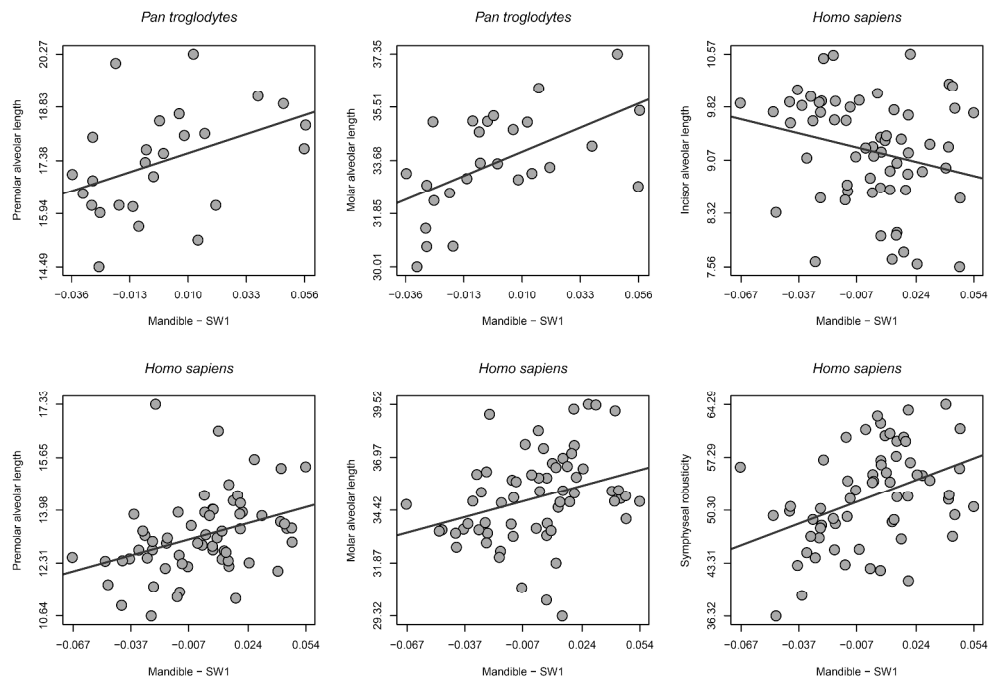
Scatterplots and linear correlations between alveolar lengths, robusticity and the pattern of neuromandibular integration (first singular warp of the mandible, SW1) in Pan troglodytes and Homo sapiens. Only the correlations that resulted significant are shown. In P. troglodytes, premolar and molar alveolar lengths increase with neurocranium length. In H. sapiens, incisor alveolar length shows an inverse relationship with neurocranium length, while postcanine alveolar lengths and symphyseal robusticity increase when the neurocranium lengthens. The R2 values of correlations are reported in Table 2. The shape variation associated with SW1 are shown in Figure 4.

1745x1222mm (96 x 96 DPI)

Table 1 Definitions of the landmarks used in this study. The landmarks from 1 to 28 belong to the mandibular configuration, from 29 to 43 to the neurocranium. (Continues to the next page).

Landmark number	Landmark Definitions
1	The buccal point at the superior tip of the septum between the mandibular central incisors.
2	The lingual point at the superior tip of the septum between the mandibular central incisors.
3	The lingual point at the superior tip of the septum between the mandibular lateral incisor and the canine (I_2/C).
4	The buccal point at the superior tip of the septum between the mandibular lateral incisor and the canine (I_2/C).
5	The buccal point at the superior tip of the septum between the mandibular canine and the first premolar and closest to the premolar (C/P_3).
6	The lingual point at the superior tip of the septum between the mandibular canine and the first premolar and closest to the premolar (C/P_3).
7	The buccal point at the superior tip of the septum between the mandibular third premolar and the fourth premolar (P_3/P_4).
8	The lingual point at the superior tip of the septum between the mandibular third premolar and the fourth premolar (P_3/P_4).
9	The buccal point at the superior tip of the septum between the mandibular fourth premolar and the first molar (P_4/M_1).
10	The lingual point at the superior tip of the septum between the mandibular fourth premolar and the first molar (P_4/M_1).
11	The buccal point at the superior tip of the septum between the mandibular first molar and the second molar (M_1/M_2).
12	The lingual point at the superior tip of the septum between the mandibular first molar and the second molar (M_1/M_2).
13	The buccal point at the superior tip of the septum between the mandibular second molar and the third molar (M_2/M_3).
14	The lingual point at the superior tip of the septum between the mandibular second molar and the third molar (M_2/M_3).
15	The most posterior point of the tooth row between the mandibular third molar septum and the retro-molar sulcus.
16	The most inferior point of the mandibular symphysis on the mid-sagittal plane.
17	The mid-sagittal point on the mandibular inferior transverse torus projecting most posteriorly.
18	The mid-sagittal point on the mandibular superior transverse torus projecting most posteriorly.

Table 1 (Continued)

Landmark number	Landmark Definitions
19	The most anterior point on the rim of the mental foramen.
20	The most inferior point of the gonial region, at the inferior margin of the masseteric fossa.
21	The most superior point of the gonial region, at the most posterior margin of the masseteric fossa.
22	The point at which the minimum mandibular ramus breadth intersects the anterior border of the ramus.
23	The most superior point, or tip, of the coronoid process.
24	The point on the mandibular notch situated medially between the tip of the coronoid process and the line connecting the most external points on the mandibular condyle.
25	The most anterior point of the mandibular condyle.
26	The interior most lateral point of the mandibular condyle.
27	The exterior most lateral point of the mandibular condyle.
28	The most posterior point of the mandibular condyle.
29	Glabella, or the most anterior and prominent point on the frontal bone, situated on the sagittal plane, between the superciliary arches and above the root of the nasal bones.
30	Bregma, or the point where the coronal suture is intersected perpendicularly by the sagittal suture.
31	Lambda, or the point where the sagittal and lambdoid suture of the skull intersect each other.
32	Inion, the most projecting point on the external occipital protuberance, or the most prominent projection of the posteroinferior region of the occipital bone.
33	Opisthion, or the most posterior point on the margin of the foramen magnum, positioned along the sagittal plane.
34	The most inferior point on the suture between the maxilla and the zygomatic bone.
35	Jugale, or the point at the union of the frontal and temporal processes of the zygomatic bone.
36	The most posterior point of the zygomaticofrontal suture, where the frontal bone meets the process of the zygomatic, on the external margin of the orbit.

1
2
3
4
5
6
7
8
9
10
11
12
13
14
15
16
17
18
19
20
21
22
23
24
25
26
27
28
29
30
31
32
33
34
35
36
37
38
39
40
41
42
43
44
45
46
47
48
49
50
51
52
53
54
55
56
57
58
59
60

Table 1 (Continued)

Landmark number	Landmark Definitions
37	Frontotemporale, or the most anterior point of the temporal line on the frontal bone.
38	The point of intersection between the coronal suture and the inferior temporal line.
39	The most posterior point of the inferior temporal line, located onto the parietal bone.
40	Asterion, or the point where the parietal, occipital and temporal bones converge.
41	The most external point of the supramastoid crest.
42	Porion, or the uppermost point on the external auditory meatus.
43	On the temporal bone, the most posterior and concave point on the internal side of the zygomatic arch.

Table 2 Results of the Redundancy Analysis to assess the contributions of neuro-mandibular integration (**NM**) to the variance of mandibular shape (PC scores), alveolar lengths (I_1-I_2, P_3-P_4 and M_1-M_3) and robusticity indices (Rob SY, M_1 and M_2). The shared (including the effect of sex and size, **NM** x **Sex** x **Size**) and unique contribution (**NM | Sex** x **Size**) of NM are reported. In addition, the table shows the contribution of sex and size to the variance explained by NM (**Sex** x **Size | NM**). The contributions are expressed as percentage of the total variance. Significant p-values are shown in bold.

	Pan troglodytes			
	NM x Sex x Size	NM | Sex x Size	Sex x Size | NM	p-value
Mandible shape	17 %	17 %	≈ 0 %	**0.001**
I_1-I_2	6 %	3 %	3 %	0.197
P_3-P_4	26 %	23 %	3 %	**0.004**
M_1-M_3	38 %	38 %	≈ 0 %	**0.002**
Rob SY	2 %	≈ 0 %	2 %	0.822
Rob M_1	≈ 0 %	≈ 0 %	≈ 0 %	0.957
Rob M_2	≈ 0 %	≈ 0 %	≈ 0 %	0.749

	Homo sapiens			
	NM x Sex x Size	NM | Sex x Size	Sex x Size | NM	p-value
Mandible shape	16 %	16 %	≈ 0 %	**0.001**
I_1-I_2	5 %	5 %	≈ 0 %	**0.046**
P_3-P_4	13 %	12 %	1 %	**0.002**
M_1-M_3	8 %	7 %	1 %	**0.018**
Rob SY	17 %	17 %	≈ 0 %	**0.002**
Rob M_1	3 %	3 %	≈ 0 %	0.111
Rob M_2	1 %	1 %	≈ 0 %	0.241